JEODEZİ VE JEOİNFORMASYON DERGİSİ
JOURNAL OF GEODESY AND GEOINFORMATION
ISSN : 2147-1339
e-ISSN: 2667-8519

Araştırma Makalesi / *Research Article*
Yıl / *Year:* 2026 **Cilt** / *Volume:* 13 **Sayı** / *Issue*: 1
Sayfa / *Page*: 33-48
Dergi No / *Journal No*: 123
Doi: 10.9733/JGG.2026R0002.E

UAV flight path impacts on three-dimensional photogrammetric product accuracy

Hasan Dilmac[1*], Veli Ilci[1], Nazime Tilbe Sasmaz[1], Fazli Engin Tombus[2]

[1]*Ondokuz Mayis University, Department of Geomatics Engineering, Samsun, Türkiye.*

[2]*Department of Survey and Cadastre, Vocational School of Technical Sciences, Hitit University, Çorum, Türkiye.*

Abstract: *The accuracy of unmanned aerial vehicle (UAV) products is affected by many parameters, such as ground control points (GCPs), flight plans, overlap rates, flight altitude, etc. Flight patterns could be another factor that influences UAV product accuracy, but is not given as much attention in the literature. The impact of seven combinations derived from Single (S), Double (D), and Circular (C) flight patterns on point formation is analysed in this study. It was also evaluated the positional accuracy and number of points in both horizontal and vertical planes within three-dimensional (3D) models. For each model, 15 common comparison surfaces (CSs) (10 vertical and 5 horizontal) were selected, and a point cloud generated by a robotic total station was used as a reference to generate reference planes (RPs), which were utilized to compute surface scoring and root mean square (RMS) error of the models. Ultimately, two separate analyses were conducted. Each model's demonstration level of the chosen horizontal and vertical planes is rated in the first analysis. In the subsequent analysis, the RMS values were determined based on the distance between the model points and the generated RPs. The study's results indicate that the D pattern offers the best option for only one flight. Furthermore, the D+C flight combination yielded the best results among the evaluated models when multiple flights were conducted.*

Keywords: UAV photogrammetry, Flight patterns, Surface extraction

İHA uçuş güzergahı şekillerinin üç boyutlu fotogrametrik ürün doğruluğuna etkisi

Öz: *İnsansız hava araçları (İHA) ile elde edilen ürünlerin doğruluğu, yer kontrol noktaları, uçuş planları, bindirme oranları, uçuş yüksekliği gibi birçok parametreden etkilenmektedir. Uçuş desenleri de İHA ürün doğruluğunu etkileyebilecek başka bir faktör olabilir, ancak literatürde bu konuya çok fazla önem verilmemiştir. Bu çalışmada, Tekli (S), Çiftli (D) ve Dairesel (C) uçuş desenlerinden türetilen yedi kombinasyonun nokta oluşumu üzerindeki etkisi incelenmiştir. Ayrıca üç boyutlu (3B) modellerde seçilen yatay ve düşey düzlemlerin konumsal doğruluk ve nokta sayıları da değerlendirilmiştir. Her model için 15 ortak karşılaştırma yüzeyi (10 düşey ve 5 yatay) seçilmiş ve referans düzlemleri (RD'ler) oluşturmak için robotik total station tarafından üretilen nokta bulutu referans olarak kullanılmıştır. Bu RD'ler, modellerin yüzey puanlaması ve karesel ortalama hatasının (KOH) hesaplanmasında kullanılmıştır. Sonuç olarak iki farklı analiz gerçekleştirilmiştir. İlk analizde, seçilen yatay ve düşey düzlemlerin her modeldeki temsil seviyesi derecelendirilmiştir. İkinci analizde ise model noktaları ile üretilen RD'ler arasındaki mesafeye dayalı KOH değerleri hesaplanmıştır. Çalışmanın sonuçları, tek uçuş için D deseninin en iyi seçeneği sunduğunu göstermektedir. Ayrıca, ikili uçuşlar için D+C kombinasyonu değerlendirilen modeller arasında en iyi sonuçları vermiştir.*

Anahtar Sözcükler: İHA fotogrametrisi, Uçuş desenleri, Yüzey çıkarımı

* Sorumlu Yazar/Corresponding Author: Tel: +90 362 319 1919/7635

0000-0001-6877-8730, hasan.dilmac@omu.edu.tr (Dilmac H.)*
0000-0002-9485-874X, veli.ilci@omu.edu.tr (Ilci V.)
0009-0002-5042-2837, tilbe.sasmaz@gmail.com (Sasmaz N. T.)
0000-0002-2607-3211, fengintombus@hitit.edu.tr (Tombus F. E.)

Geliş Tarihi/Received: 30.09.2025
Kabul Tarihi/Accepted: 24.11.2025

1. Introduction

With the development of Structure-from-Motion (SfM) technology, unmanned aerial vehicles (UAVs) equipped with non-metric digital cameras have become rapidly developing tools for constructing 3D models of objects (Varbla et al., 2021; Yang et al., 2013). There are two steps to the 3D topography reconstruction using UAVs. The UAVs' cameras take a series of pictures of the terrain as the initial step. Afterwards, feature extraction, point matching, and the vision system's prior knowledge are combined by SfM to enable a 3D model (Byrne et al., 2017).

Software that can handle these steps and whose functionality has been demonstrated in several studies includes packages such as Pix4DMapper, Photoscan, DJI Terra and ContextCapture (V. Casella et al., 2020; Jeon et al., 2017; Kameyama & Sugiura, 2021; Mitka et al., 2023). UAVs offer distinct advantages over satellite-based remote sensing and conventional piloted aircraft, particularly in terms of cost, operational flexibility, and improved temporal and spatial resolution. They now have more civil uses thanks to their recent significant advancements and the production of microsensors (Agüera-Vega et al., 2017; Colica et al., 2021). In the literature, there are various and well-documented research based on UAVs: 3D modelling and virtual reconstruction of archaeological sites (Carvajal-Ramírez et al., 2019; Waagen, 2019); documenting of building facades (Roca et al., 2013; Russo et al., 2019); disaster damage estimation (Dominici et al., 2017; Kakooei & Baleghi, 2017); cultural heritage documentation (Bakirman et al., 2020); monitoring of road condition (Roberts et al., 2020); change detection in river topography and vegetation (Watanabe & Kawahara, 2016); landslide mapping (Gupta & Shukla, 2018); coastal change monitoring (Gonçalves & Henriques, 2015); precise agriculture (Messina et al., 2020), etc.

One advantage of UAV-borne sensors is the capacity to collect data at close range from various angles of view. UAV surveys are typically nadir, meaning the camera axis is vertically aligned. This allows for a forward overlap between shots as well as a side overlap between lanes, enabling a 3D reconstruction of the surveyed area or object (Vacca et al., 2017). However, this kind of survey ignores the 3D geometry of a scene. Specifically, they are not the best for recording features exposed along vertical facades because these features are more likely to be excluded from nadir-view sensors or to deform more than other features (Nesbit & Hugenholtz, 2019). Recently, oblique photogrammetry, in which the camera axis is at an angle with respect to the vertical, has gained a lot of attention. It captures more of the side structure of the target, thereby overcoming the drawbacks of nadir photography (Lin et al., 2021).

After exporting the final outputs (point cloud, DSM, etc.), it's vital to assess the accuracy of the photogrammetric project. The root mean square (RMS) is generally used to evaluate the accuracy (Martínez-Carricondo et al., 2018) of UAV photogrammetry determined by a wide range of factors, such as flight plan, camera image quality, camera modelling technique, SfM algorithms, ground control points (GCPs), and georeferencing strategy. In addition to maintaining a consistent height over the ground and uniform coverage over the whole region, the flight plan should incorporate sufficient forward and side overlaps (Sanz-Ablanedo et al., 2018; Zhao et al., 2021). Mesas-Carrascosa et al. (2016) analyze the influences of flight parameters such as flight altitude, forward and side overlaps on orthomosaics and suggest higher percentages of forward and side overlap for UAV flights. Akturk and Altunel (2019) focus on the accuracy assessment of the digital elevation model (DEM) generated by low-cost UAVs in challenging terrain and the influences of GCPs. Their findings showed the total error at z values was reduced by 6 cm with the addition of GCPs.

GCPs are typically used to georeference the 3D point cloud produced during the photogrammetric process. The control points for the flight might be either fixed ground features or pre-flight reference targets dispersed throughout the ground. Their exact coordinates must be surveyed as accurately as possible to improve the model. Georeferencing requires a minimum of three

GCPs; however, to enhance the accuracy of the photogrammetric outputs, it is highly recommended to increase the number of GCPs (Ferrer-González et al., 2020). Most of the studies conducted about the accuracy of UAV photogrammetry products are related to GCP, flight altitude, and overlap rates (E. Casella et al., 2020; Elkhrachy, 2021; Frey et al., 2018; Liu et al., 2022; Ridolfi et al., 2017; Turk et al., 2025).

Except for these parameters, flight patterns may influence the accuracy of the output. Various flight patterns can be created based on the dimensions of the study area and the required data. In the field of earth sciences, on the other hand, the most common patterns for flight lines are either double grid (also known as perpendicular) or single grid (also known as lawnmower) (Chaudhry et al., 2020). Furthermore, a circular flight plan is also employed, in which the UAV captures images from all angles around an object (Chiabrando et al., 2017; Zhang et al., 2020).

While previous studies have generally examined the effects of GCP distribution, flight altitude, and image overlaps on UAV photogrammetry accuracy, the impact of different flight patterns has not been thoroughly examined. The aim of this study is to fill this gap by systematically analyzing how various UAV flight patterns and their combinations influence the accuracy of 3D models. The primary research question of this work is how different UAV flight patterns affect point cloud formation and the resulting model accuracy in horizontal and vertical planes. To address this question, an experiment was conducted in an area of approximately 10 hectares, featuring various structures such as trees, buildings, and parking areas, to test the accuracy of models based on different flight patterns and their combinations.

Three flight patterns: Single (S), Double (D), and Circular (C), with nadir and oblique axes, were flown. Seven combinations of these flights (S, D, C, S+D, S+C, D+C, and S+D+C) were processed, and 3D models were produced. Reference Planes (RPs) were extracted from a reference point cloud generated using a highly sensitive robotic total station to test the accuracy of the models. A total of 15 comparison surfaces (CSs) were determined on building facades, parking areas, and roads. Two analyses were conducted: one based on the distribution and number of points on the CSs, and the other on the RMS values of distances between the points and RPs, to determine how accurately the points in the models represent RPs. As a result, the impact of flight patterns on point formation and accuracy in horizontal and vertical planes was examined.

The models in this study were processed using Pix4Dmapper, which provides a stable workflow for UAV-based image processing. While different software, such as Photoscan, ContextCapture, or DJI Terra, may apply distinct image matching and dense point cloud generation algorithms, previous studies (Aicardi et al., 2016; Jeon et al., 2017) have shown that such differences mainly affect the absolute accuracy rather than the relative performance among models. In this context, comparing different flight patterns made with the same study area and UAV platform provides a more objective comparison plane by minimizing the impact of environmental and software variations. Nevertheless, future studies could further validate these findings using alternative software to better understand potential software-based variations in reconstruction accuracy and point density.

2. Materials and Methods

2.1 Study Area

The study site is a 10.37 ha area located on the Ondokuz Mayis University Campus in Samsun, Türkiye (Figure 1). The site includes two buildings of the Engineering Faculty, which are 6 and 2 floors high. Apart from the buildings, the area features roads, parking lots, and green spaces with small trees.

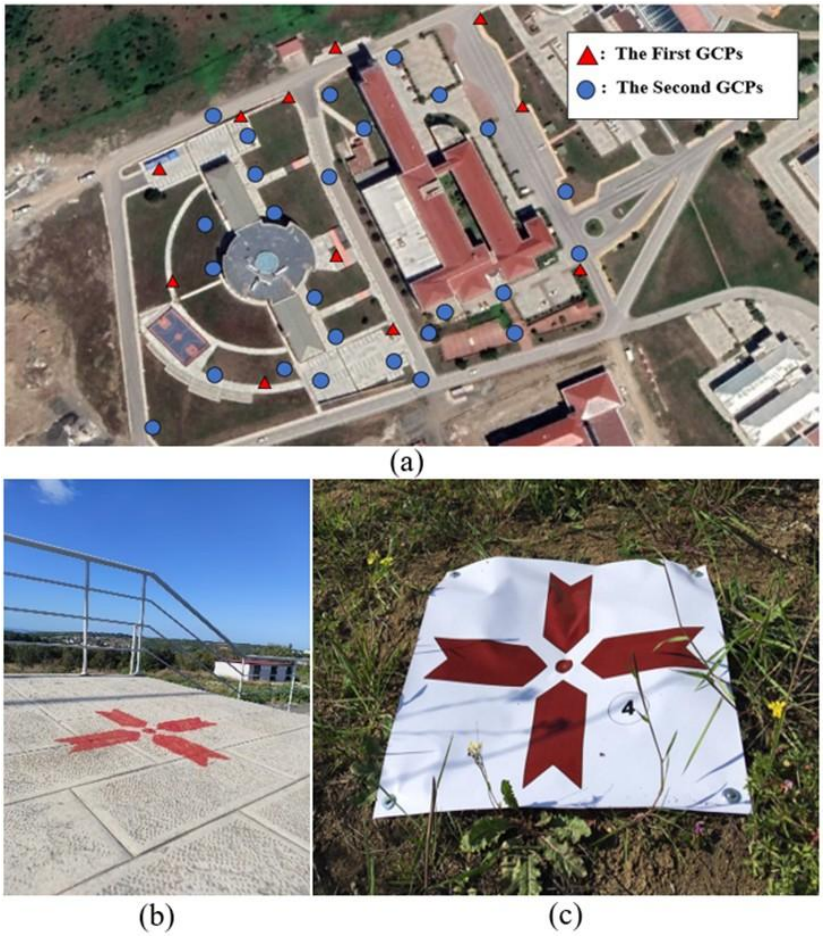

Figure 1: *Study area (a) the distribution of GCPs, (b) the first group of GCPs, (c) the second group of GCPs*

2.2 Ground Control Points

A total of 37 GCPs used for geo-referencing are divided into two groups:

- The first GCP group consists of 11 permanent points on the ground distributed systematically across the study area (red triangles in Figure 1a). Metal screws were installed into the ground and painted red (Figure 1b). Four hours of static GNSS observations were conducted using Topcon HiperPro multi-frequency GNSS receivers. The static GNSS observations were processed using the Grafnet static baseline processor and network adjustment package (URL-1). The continuously operating reference stations' static data, updated at 1-second intervals, serves as a reference for static processes. Highly accurate and reliable position information was obtained in the ITRF96 datum – 2005.0 epoch at these GCPs.

- The second GCP group consists of 26 temporal points on the ground (blue circles in Figure 1a) made from vinyl (Figure 1c). These points were located in the field for densification aim where the first GCP group points were sparse. These points' coordinates were determined with 1-2 cm-level accuracy by using Topcon HiperV based on the real-time kinematic (RTK) GNSS observation technique.

2.3 Data Acquisition with UAV

We used the DJI Phantom 4 Pro UAV equipped with a 1-inch CMOS 20-megapixel sensor for the flights (URL-2). Three flight patterns —Single, Double, and Circular — were applied (Figure 2).

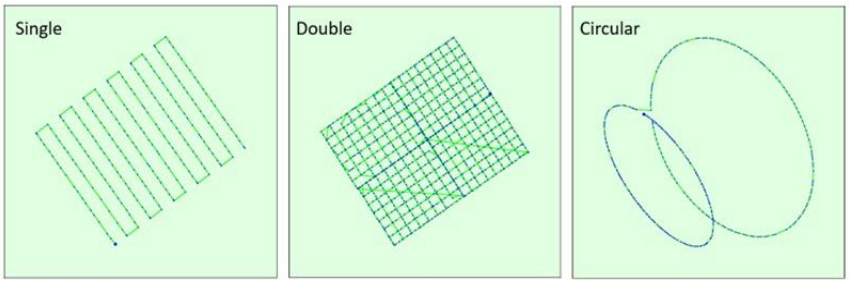

Figure 2: *Flight patterns (URL-3)*

One flight of 14 minutes was sufficient to cover the area with a Single pattern at a nadir angle. Four flights lasting a total of 60 minutes were made with a Double pattern at an oblique angle. In the Circular pattern, two flights were conducted for two buildings, each lasting 8 minutes. Additionally, some flight parameters, such as altitude, camera angle, and overlap rates, are listed in Table 1.

Table 1: *UAV flight plan parameters*

Flight mission	Altitude (m)	The angle of the camera (degree)	Front overlap (%)	Side overlap (%)	Duration (min)	Number of flights
Single grid (S)	60	90	80	70	14	1
Double grid (D)	40	60	80	70	60	4
Circular (C) building 1 / 2	40 / 30	45 / 45	-	90 / 90	8 / 8	2

2.4 Flight Data Processing

We used Pix4Dmapper photogrammetry software for the processes (URL-3). The collected UAV flight data from three flight patterns were processed in seven variations (Table 2). The same hardware was used for all processes.

Table 2: *The number of photographs used and processing outputs*

Processes	Number of photographs	GSD* of sparse point cloud (cm/pixel)	Number of GCPs	RMS error (cm)	Process duration
Single (S)	244	1.59	37	5.0	0d 12h 09m 32s
Double (D)	1056	1.24	37	2.4	0d 20h 16m 37s
Circular (C)	295	6.20	37	3.5	0d 07h 16m 40s
S + D	1300	1.33	37	2.5	0d 22h 07m 36s
S + C	539	1.80	37	2.6	0d 18h 15m 57s
D + C	1351	1.33	37	2.5	0d 23h 01m 10s
S + D + C	1595	1.41	37	2.4	1d 00h 33m 11s

* GSD: Ground sampling distance

The ground sampling distance (GSD), which is directly dependent on parameters such as flight altitude and camera angle, is a critical parameter in UAV-based mapping studies (Mesas-Carrascosa et al., 2016). This variable significantly affects both the amount of data produced and the total flight time. This is convenient for Table 2 results, considering the flight durations in Table 1. Because of the circular and single processes, the RMS errors may seem confusing at first glance; however, the single process generated seven times more points than the circular process. So, the RMS errors and point numbers should be considered together. The point number is as significant as the RMS errors because it gives more detailed and softer environmental information (Figure 3).

Figure 3: *Obtained models with processing types (point numbers are given in parentheses)*

2.5 Reference Data Collection

A Leica TS16 robotic total station was used to scan the building surfaces and the ground (URL-4). This automatic total station delivers highly accurate and reliable angle and distance measurements in any environmental circumstances. The robotic total

station was set to the 11 permanent GCPs that were determined by static processing, and a reference point cloud was obtained (Figure 4). The surfaces were scanned with a spacing between 0.2 and 0.5 grads in horizontal and vertical angles. These values have been determined by considering the time and energy consumption, as well as the best representation of the target surfaces.

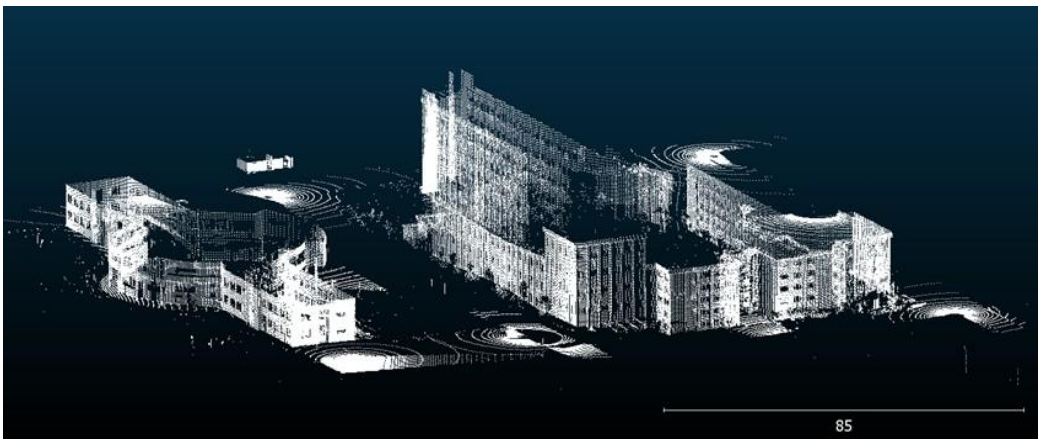

Figure 4: *Reference point cloud*

To test the accuracy of the processes, 15 CSs were equally distributed across the study area, with 5 in the horizontal plane (H1, H2, …, H5) and 10 in the vertical plane (V1, V2, …, V10) (Figure 5). CloudCompare software was used for point cloud operations (URL-5).

Figure 5: *Comparison surfaces*

CSs were chosen from the facades of buildings for vertical accuracy evaluation (Figure 6) and from roads and parking areas for horizontal accuracy evaluation (Figure 7). The horizontal CSs were selected close to the total station with the highest point density. Then, RPs are obtained by fitting a plane to the points in CSs from the reference point cloud. Plane fitting was performed using the least squares method implemented in CloudCompare. In this approach, the most suitable plane is determined by minimizing the sum of the squares of the perpendicular distances between the plane surfaces and the points. Additionally, the RMS fitting error reported by CloudCompare was used as an indicator of local surface accuracy. RMS values of RPs are in the range of 0.3-1.8 cm (Table 3).

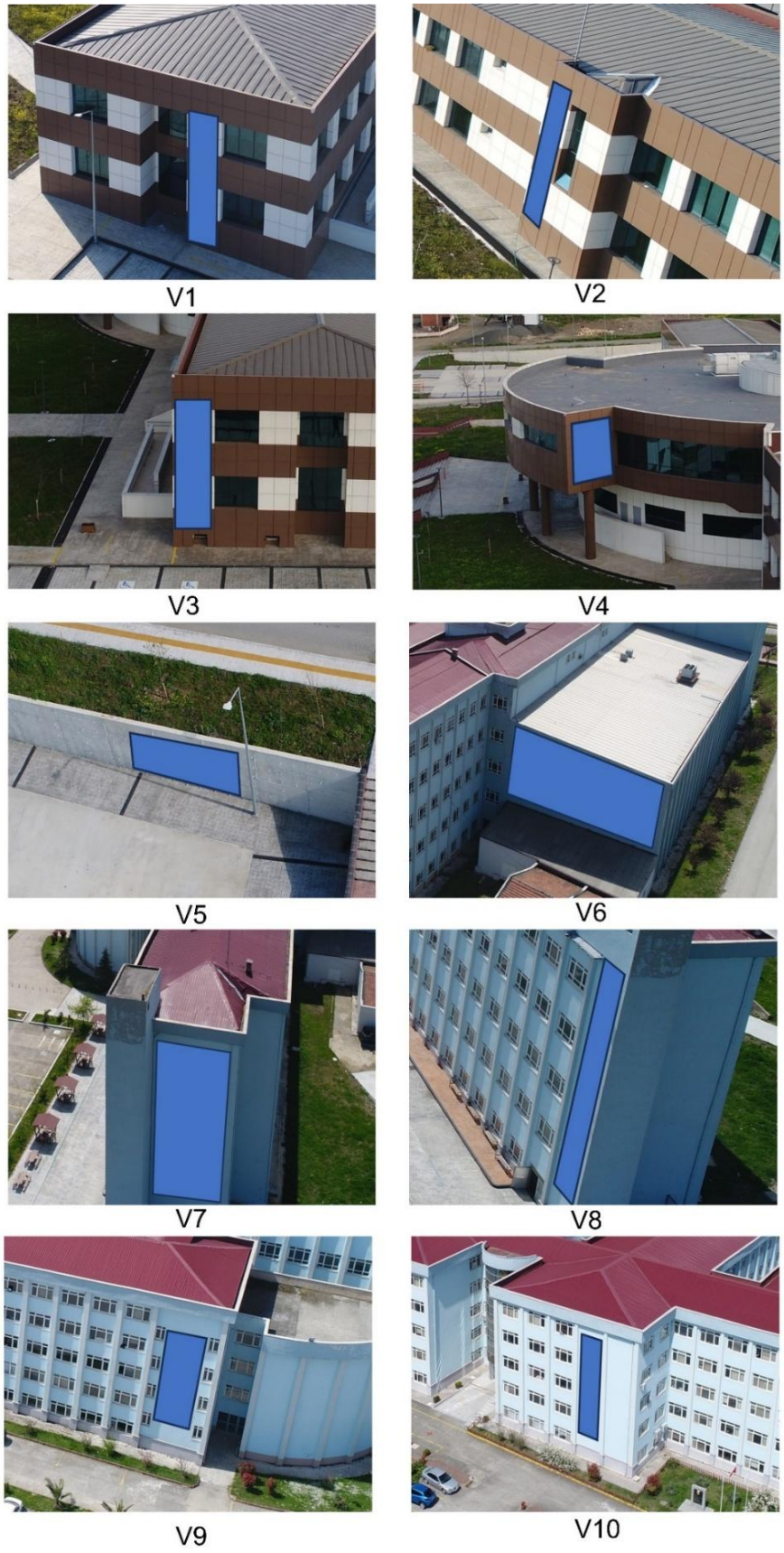

Figure 6: *Vertical RPs*

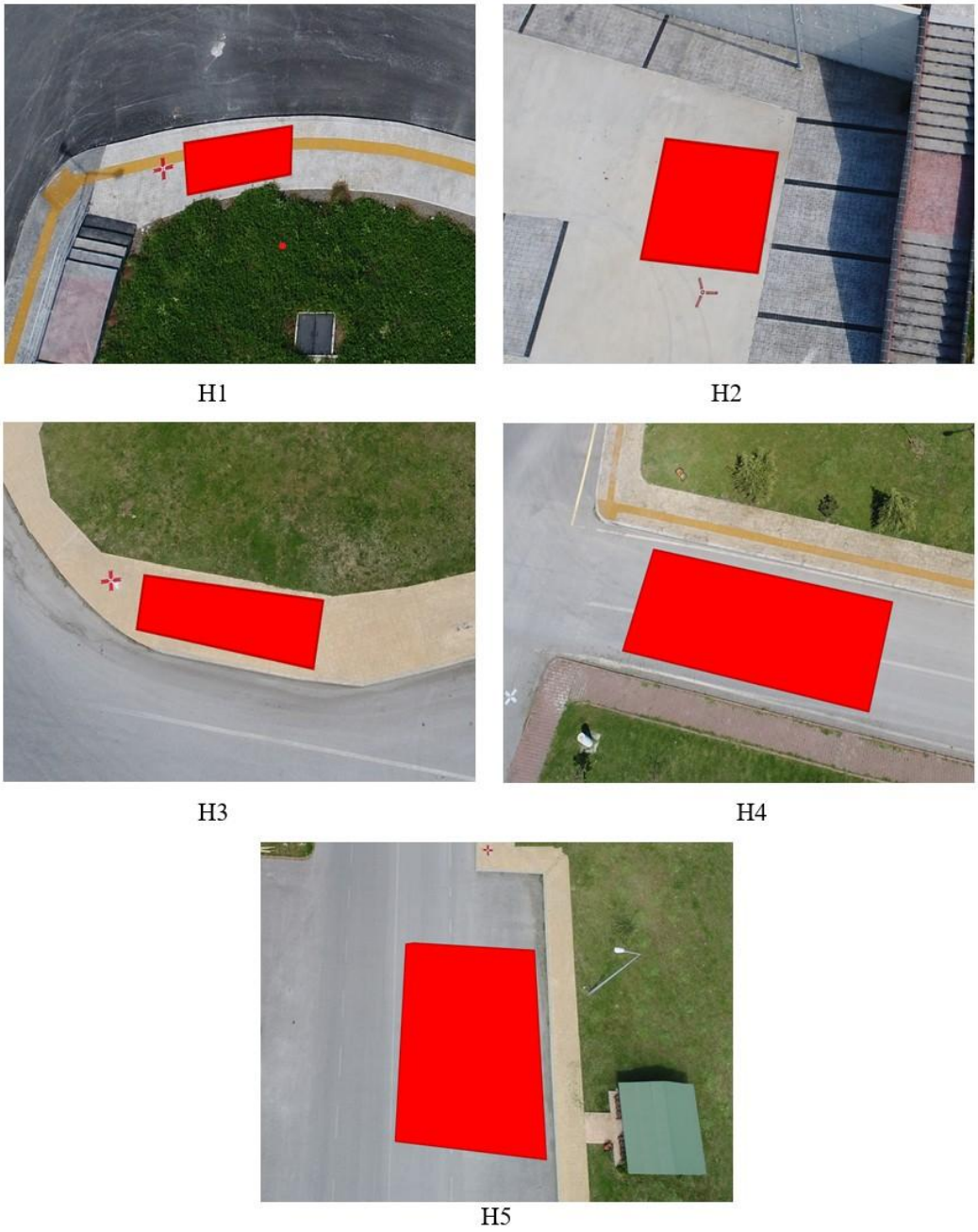

Figure 7: *Horizontal RPs*

Table 3: *RMS values of RPs*

RP	RMS (cm)	RP	RMS (cm)
H1	0.6	V1	0.3
H2	0.3	V2	0.3
H3	1.2	V3	0.7
H4	1.3	V4	0.4
H5	0.7	V5	0.4
		V6	1.3
		V7	0.8
		V8	1.8
		V9	0.7
		V10	0.7

3. Results and Discussion

To compare the accuracy of point clouds created by UAV photogrammetry across different flight and processing types, seven distinct point cloud models were generated. A point cloud created using a terrestrial scanning system was used for reference. Two different analyses were carried out. The first analysis evaluates how well each model represents the selected horizontal and vertical planes. Five-point density criteria were established in this respect, and scores were assigned to these surfaces on a scale of 0 to 4 (Figure 8).

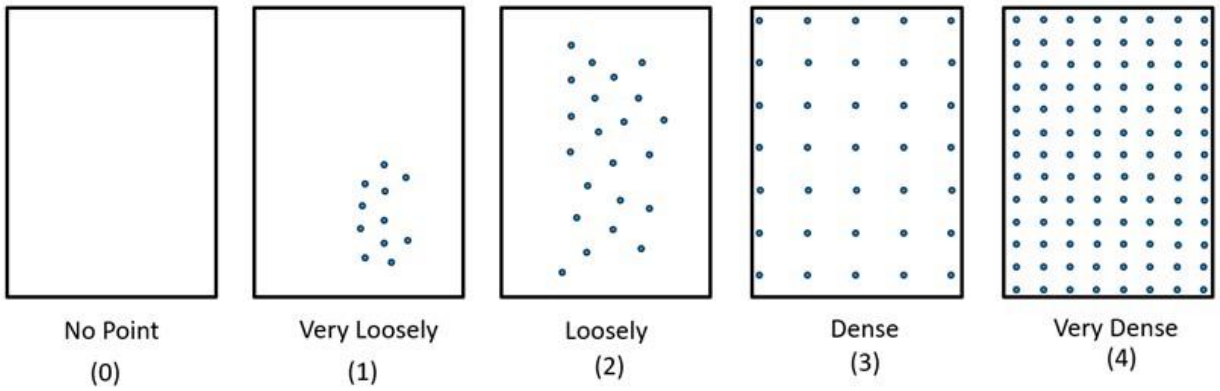

Figure 8: *Scoring scale*

To compare the results of the first analysis, the scores of all processes in both horizontal and vertical planes were considered in three different ways. Firstly, the sum of all horizontal plane scores of each process is named as total H for horizontal evaluation; secondly, the sum of all vertical plane scores of each process is named as total V for vertical evaluation; and lastly, the sum of all scores of each process was taken for a general assessment. Compared to other processes, the single-process results were below average in total. However, when looking at the total H value, it received the maximum score possible. It has been observed that the single process is generally inadequate because its performance in vertical planes remains relatively low. The double process received almost the highest score on all surfaces. However, its performance in the V7 and V8 planes is low compared to the other planes because the flight route is very close to the buildings at that point. The circular process received an above-average score. But, unlike the single process, this method performs poorly in horizontal planes. S+D and S+C processes produced nearly identical results to the Double process, except for V7 and V8 planes. The D+C process received the highest score on almost all surfaces. The S+D+C process received maximum scores on every surface, both horizontally and vertically. As a result of the scoring, it was seen that the S + D + C process gave the best results on all surfaces. Then, D+C followed it very closely, followed by S+D, D, S+C, C, and S, respectively (Table 4).

Table 4: *The results of surface scoring*

Process	H1	H2	H3	H4	H5	V1	V2	V3	V4	V5	V6	V7	V8	V9	V10	Total
S	4	4	4	4	4	1	2	1	0	2	1	1	2	3	1	34
D	4	4	4	4	4	4	4	4	3	4	4	1	2	4	4	54
C	2	4	3	4	3	4	2	4	4	3	4	3	3	3	3	49
S + D	4	4	4	4	4	4	4	4	3	4	4	2	2	4	4	55
S + C	4	4	4	4	3	4	2	4	4	3	4	3	3	4	3	53
D + C	4	4	4	4	4	4	4	4	4	4	4	3	3	4	4	58
S + D + C	4	4	4	4	4	4	4	4	4	4	4	3	4	4	4	59

Heat maps were created to better visualize the distribution of surface scores (Figures 9 and 10). The D+C and S+D+C processes consistently demonstrated high scores, confirming their high-quality restructuring performance.

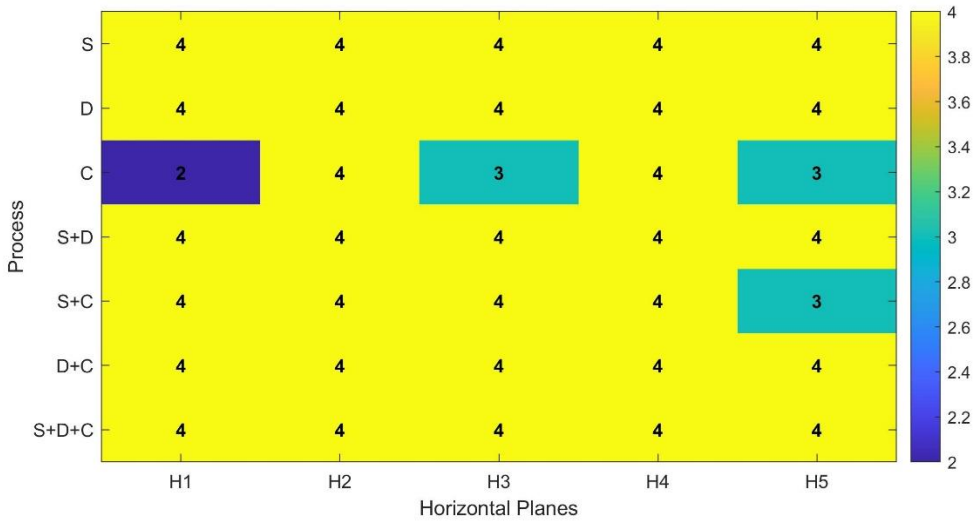

Figure 9: *Heat map of surface scoring results for horizontal planes*

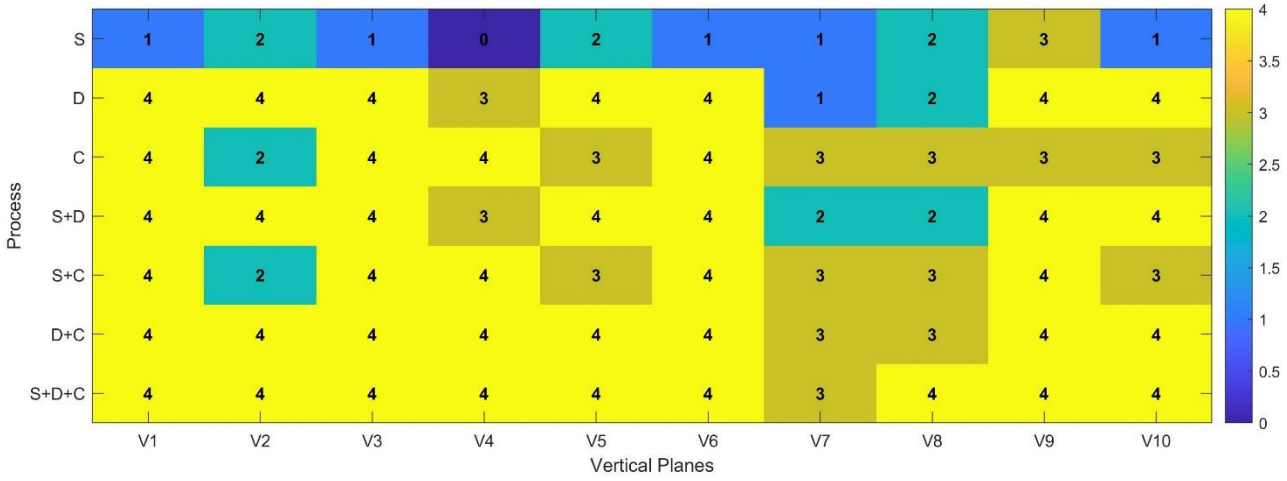

Figure 10: *Heat map of surface scoring results for vertical planes*

In the second analysis, RMS values were calculated based on the distance of the points in the models from the RPs (Table 5). The single process delivered very precise and cm-level results in horizontal planes. However, it generally did not provide accurate results in vertical planes and was unable to produce any data in the V4 plane. In general, its accuracy remained at the dm-level in vertical. The double process generally offered results with cm-level in both horizontal and vertical planes. However, its accuracy decreased to the dm-level in the V7 and V8 planes. All processes except the Circular process generally generated accurate results in horizontal planes. The Circular process yielded results at the dm level in horizontal planes. The combined processes (S+D, S+C, D+C, and S+D+C) produced similar overall accuracies, with minor variations. However, the number of points in the planes is also significant in terms of evaluating RMS values. While the Single process delivered a very high number of points in most horizontal planes, it was generally below the average in vertical planes. The double process generally yielded a high number of points in both horizontal and vertical planes. The circular process produced the lowest number of points in horizontal planes. Generally, processes, including the circular process, have low points in horizontal planes. However, the D+C process showed an exception at this point. S+D, D+C, and S+D+C processes had high points in both horizontal and vertical planes (Table 6).

Table 5: *The RMS values (cm) of the distances between processing models and reference planes*

Process	H1	H2	H3	H4	H5	Mean RMS	V1	V2	V3	V4	V5	V6	V7	V8	V9	V10	Mean RMS
S	4	4	3	4	2	3.4	10	7	4	-	7	25	6	10	12	13	11.9
D	2	2	1	2	1	1.6	6	6	4	7	2	5	18	8	8	5	6.9
C	13	3	4	10	4	6.8	5	7	4	5	7	13	17	9	6	9	8.2
S + D	2	2	1	2	1	1.6	5	6	4	7	3	8	17	7	7	4	6.8
S + C	3	2	3	6	3	3.4	5	7	4	4	5	14	17	6	6	8	7.6
D + C	2	2	2	3	2	2.2	5	6	3	6	3	10	21	13	7	6	8.0
S + D + C	3	2	2	4	2	2.6	6	5	4	6	4	6	21	10	7	6	7.5

Table 6: *The number of points on horizontal and vertical planes*

Process	H1	H2	H3	H4	H5	V1	V2	V3	V4	V5	V6	V7	V8	V9	V10
S	20475	28604	37174	32409	101334	193	1020	204	0	1239	16416	514	4029	6215	377
D	10883	18347	17759	27319	96612	3865	2669	5222	5624	7123	75416	752	5673	11065	11988
C	175	5857	2853	4584	30317	4122	567	9213	8627	1074	37835	10242	3239	3352	3347
S + D	12860	20694	23632	32286	121187	4043	2959	4933	6338	7792	86784	1748	3467	10703	10693
S + C	3224	9406	7913	11404	54855	6291	753	7393	6111	1781	42846	10829	2849	4726	2855
D + C	11205	22693	21262	29555	150242	7854	2937	9459	11331	7761	78428	12759	10220	12635	12941
S + D + C	13524	25492	27426	31397	170405	7757	2850	10231	13052	8003	89982	10709	10165	13943	10642

3.1 Statistical Analysis of the Results

To assess whether the differences observed in surface scoring and RMS-based analyses were statistically significant, a one-way analysis of variance (ANOVA) was used. The test was performed using the *anova1* function in MATLAB with a default significance level of 0.05. ANOVA tests were performed separately for horizontal and vertical planes based on the results in Tables 4 and 5. The ANOVA results revealed statistically significant differences between the models in terms of point formation in both horizontal and vertical planes; the p-values were 0.01 and 1.6×10^{-9}, respectively. In contrast, when ANOVA was applied to RMS-based results, statistically significant differences were observed only for horizontal planes ($p = 0.02$), and no significant difference was found for vertical planes ($p = 0.73$).

Statistical tests indicate that flight patterns and processing types have a significant impact on point formation, as reflected in surface scoring results, and that both horizontal and vertical planes exhibit significant differences. This affects the overall representation quality across all planes. In contrast, RMS-based analysis revealed significant differences only in the horizontal plane, while changes in the vertical plane were not statistically significant. This may indicate that, although the models differ in terms of point distribution density (scoring), the deviations of the points from the reference planes are more consistent in the vertical direction. In other words, while horizontal accuracy is more sensitive to the choice of flight-processing strategy, vertical accuracy remains relatively constant across the tested models.

A potential concern regarding this study is that the flight patterns were performed in different flight configurations; this could affect the accuracy of the photogrammetric outputs. However, these differences primarily stem from the unique flight geometry requirements of each pattern. Although such variations could potentially affect model accuracy, their impact is not expected to be significant. Phojaem et al. (2025) systematically investigated the effect of flight altitude, camera angle, and overlap percentage on RMSE across 27 UAV configurations. Their results showed that lower altitudes and higher overlaps generally improved spatial accuracy (e.g., RMSE increased from 2.30 cm at 30 m to 3.37 cm at 60 m, and deteriorated below 60% overlap); however, these effects were found to be within a few centimeters and primarily due to image redundancy. Therefore, within the relatively narrow parameter ranges adopted in this study, changes in height, overlap, and camera angle

may cause marginal accuracy differences; however, these are unlikely to cause systematic or significant degradation in the final reconstruction. Thus, these parameter differences do not systematically correspond to the accuracy variations observed between different flight configurations and cannot fully explain the larger inconsistencies reported in this study.

4. Conclusion

This study analyzed the positional accuracies of the models obtained using three flight patterns and various combinations of these flights in UAV photogrammetry. For reference, a robotic total station was used to create a point cloud with high precision in both angle and distance. For analysis, common horizontal and vertical CSs were selected in the models. Two different analyses were carried out to evaluate the accuracy of the models. A statistical analysis was then applied to the results to evaluate the significance of the differences.

In the first analysis, the density of points on the comparison surfaces and their plane representation levels were compared. For this purpose, the point density and distribution of the planes were scored on a scale of 0 to 4. The S process received the lowest score in vertical planes; however, it received one of the highest scores in the horizontal planes. Therefore, in an experiment where vertical details are unimportant, the S process may be preferred, considering time and labor. The D process demonstrated higher-than-average success on both horizontal and vertical surfaces. So, if favourable results are expected in both horizontal and vertical planes by using only one flight data, it is seen that the best flight pattern is D. On the other hand, if the vertical details of one object are essential, the C flight pattern may be preferred. When it comes to flight combinations, in general, dual flight combinations had very accurate results. However, the D+C combination gave the best result among the dual combinations. Therefore, D and C flights should be preferred if a two-flight is to be made. Although the S+D+C process produced the best results, implementing the three flight patterns is the most demanding in terms of time and labor. Additionally, when comparing the D+C process with the S+ D+C process, no significant difference was observed in terms of positional accuracy on horizontal and vertical surfaces.

In the second analysis, the RMS values of the distances between the RPs and the model points corresponding to these planes, as well as the density of these points, were examined. The S model performs poorly in vertical planes, while the C process performs poorly in horizontal planes. Apart from that, generally all processes possess cm-level accuracies. When the average of the RMS values is taken as a criterion, the D and S+D models give the best results. However, it has been observed that although RMS values alone are sufficient to describe the accuracy of the models, they are insufficient to explain how well they define those planes. For this reason, point numbers should also be taken into account. For example, while the S process generated approximately 30,000 points in the H2 plane and had an error of 4 cm, the C process produced approximately 6,000 points in the H2 plane and had an error of 3 cm. Therefore, although its accuracy is higher than that of the single process, the score of the C process in the H2 plane is below that of the S process because it cannot fully define that plane with 6,000 points. In summary, it is impossible to obtain complete information about whether the models can determine those planes, just by using the RMS values. In this respect, the D process yielded the most optimal results when considering the processes of a single flight. If more than one flight is to be made, D and C flight combination have been observed to provide the best results among the models.

Subsequent statistical analyses also supported these results. One-way ANOVA tests confirmed statistically significant differences in surface representation for both horizontal and vertical planes. However, RMS-based results, which provide a measure of the spatial differences between model points and reference planes, found statistically significant differences only for horizontal planes. This demonstrates that flight patterns and process types have a substantial impact on point cloud models

in terms of horizontal accuracy and reconstruction capability. Vertical accuracy, on the other hand, tended to be more stable.

Author Contribution

Hasan Dilmac: Conception, Design, Literature review, Data collection, Analysis and interpretation, Writing. **Veli Ilci:** Conception, Design, Supervision, Review of article. **Tilbe Sasmaz:** Data collection, Analysis, Writing. **Fazli Engin Tombus:** Data collection, Review of article.

Declaration of Competing Interests

The authors declare that they have no known relevant competing financial or non-financial interests that could have appeared to influence the work reported in this paper.

References

Agüera-Vega, F., Carvajal-Ramírez, F., & Martínez-Carricondo, P. (2017). Assessment of photogrammetric mapping accuracy based on variation ground control points number using unmanned aerial vehicle. *Measurement, 98*, 221–227.

Aicardi, I., Chiabrando, F., Grasso, N., Lingua, A. M., Noardo, F., & Spanò, A. (2016). UAV photogrammetry with oblique images: First analysis on data acquisition and processing. *ISPRS Archives of the Photogrammetry, Remote Sensing and Spatial Information Sciences*, XLI-B1, 835–842.

Akturk, E., & Altunel, A. O. (2019). Accuracy assessment of a low-cost UAV derived digital elevation model (DEM) in a highly broken and vegetated terrain. *Measurement 136*, 382–386.

Bakirman, T., Bayram, B., Akpinar, B., Karabulut, M. F., Bayrak, O. C., Yigitoglu, A., & Seker, D. Z. (2020). Implementation of ultra-light UAV systems for cultural heritage documentation. *Journal of Cultural Heritage, 44*, 174–184.

Byrne, J., O'Keeffe, E., Lennon, D., & Laefer, D. F. (2017). 3D reconstructions using unstabilized video footage from an unmanned aerial vehicle. *Journal of Imaging, 3*(2), 15.

Carvajal-Ramírez, F., Navarro-Ortega, A. D., Agüera-Vega, F., Martínez-Carricondo, P., & Mancini, F. (2019). Virtual reconstruction of damaged archaeological sites based on Unmanned Aerial Vehicle Photogrammetry and 3D modelling. Study case of a southeastern Iberia production area in the Bronze Age. *Measurement, 136*, 225–236.

Casella, E., Drechsel, J., Winter, C., Benninghoff, M., & Rovere, A. (2020). Accuracy of sand beach topography surveying by drones and photogrammetry. *Geo-Marine Letters, 40*(2), 255–268.

Casella, V., Chiabrando, F., Franzini, M., & Manzino, A. M. (2020). Accuracy assessment of a UAV block by different software packages, processing schemes and validation strategies. *ISPRS International Journal of Geo-Information, 9*(164), 1–21.

Chaudhry, M. H., Ahmad, A., & Gulzar, Q. (2020). Impact of uav surveying parameters on mixed urban landuse surface modelling. *ISPRS International Journal of Geo-Information, 9*(11), 656.

Chiabrando, F., Lingua, A., Maschio, P., & Teppati Losè, L. (2017). The influence of flight planning and camera orientation in UAVs photogrammetry. A test in the area of rocca San Silvestro (LI), Tuscany. *International Archives of the Photogrammetry, Remote Sensing and Spatial Information Sciences - ISPRS Archives, 42*(2W3), 163–170.

Colica, E., D'Amico, S., Iannucci, R., Martino, S., Gauci, A., Galone, L., Galea, P., & Paciello, A. (2021). Using unmanned aerial vehicle photogrammetry for digital geological surveys: case study of Selmun promontory, northern of Malta. *Environmental Earth Sciences, 80*(17), 1–14.

Dominici, D., Alicandro, M., & Massimi, V. (2017). UAV photogrammetry in the post-earthquake scenario: case studies in L'Aquila. *Geomatics, Natural Hazards and Risk, 8*(1), 87–103.

Elkhrachy, I. (2021). Accuracy Assessment of Low-Cost Unmanned Aerial Vehicle (UAV) Photogrammetry. *Alexandria Engineering Journal, 60*(6), 5579–5590.

Ferrer-González, E., Agüera-Vega, F., Carvajal-Ramírez, F., Martínez-Carricondo, P. (2020). UAV photogrammetry accuracy assessment

for corridor mapping based on the number and distribution of ground control points. *Remote Sensing, 12*(15), 2447.

Frey, J., Kovach, K., Stemmler, S., & Koch, B. (2018). UAV photogrammetry of forests as a vulnerable process. A sensitivity analysis for a structure from motion RGB-image pipeline. *Remote Sensing, 10*(912), 1–12.

Gonçalves, J. A., & Henriques, R. (2015). UAV photogrammetry for topographic monitoring of coastal areas. *ISPRS Journal of Photogrammetry and Remote Sensing, 104*, 101–111.

Gupta, S. K., & Shukla, D. P. (2018). Application of drone for landslide mapping, dimension estimation and its 3D reconstruction. *Journal of the Indian Society of Remote Sensing, 46*(6), 903–914.

Jeon, E. I., Yu, S. J., Seok, H. W., Kang, S. J., Lee, K. Y., & Kwon, O. S. (2017). Comparative evaluation of commercial softwares in UAV imagery for cultural heritage recording: case study for traditional building in South Korea. *Spatial Information Research, 25*(5), 701–712.

Kakooei, M., & Baleghi, Y. (2017). Fusion of satellite, aircraft, and UAV data for automatic disaster damage assessment. *International Journal of Remote Sensing, 38*(8–10), 2511–2534.

Kameyama, S., & Sugiura, K. (2021). Effects of differences in structure from motion software on image processing of unmanned aerial vehicle photography and estimation of crown area and tree height in forests. *Remote Sensing, 13*(4), 1–22.

Lin, L., Yu, K., Yao, X., Deng, Y., Hao, Z., Chen, Y., Wu, N., & Liu, J. (2021). UAV based estimation of forest leaf area index (Lai) through oblique photogrammetry. *Remote Sensing, 13*(803), 1–16.

Liu, X., Lian, X., Yang, W., Wang, F., Han, Y., & Zhang, Y. (2022). Accuracy Assessment of a UAV Direct Georeferencing Method and Impact of the Configuration of Ground Control Points. *Drones, 6*(2), 30.

Martínez-Carricondo, P., Agüera-Vega, F., Carvajal-Ramírez, F., Mesas-Carrascosa, F. J., García-Ferrer, A., & Pérez-Porras, F. J. (2018). Assessment of UAV-photogrammetric mapping accuracy based on variation of ground control points. *International Journal of Applied Earth Observation and Geoinformation, 72*, 1–10.

Mesas-Carrascosa, F. J., García, M. D. N., De Larriva, J. E. M., & García-Ferrer, A. (2016). An analysis of the influence of flight parameters in the generation of unmanned aerial vehicle (UAV) orthomosaicks to survey archaeological areas. *Sensors, 16*(11), 1838.

Messina, G., Peña, J. M., Vizzari, M., & Modica, G. (2020). A comparison of UAV and satellites multispectral imagery in monitoring onion crop. An application in the 'Cipolla Rossa di Tropea' (Italy). *Remote Sensing, 12*(20), 1–27.

Mitka, B., Klapa, P., & Pióro, P. (2023). Acquisition and Processing Data from UAVs in the Process of Generating 3D Models for Solar Potential Analysis. *Remote Sensing, 15*(6), 1498.

Nesbit, P. R., & Hugenholtz, C. H. (2019). Enhancing UAV-SfM 3D model accuracy in high-relief landscapes by incorporating oblique images. *Remote Sensing, 11*(3), 1–24.

Phojaem, T., Dangbut, A., Wisutwattanasak, P., Janhuaton, T., Champahom, T., Ratanavaraha, V., & Jomnonkwao, S. (2025). Evaluating UAV Flight Parameters for High-Accuracy in Road Accident Scene Documentation: A Planimetric Assessment Under Simulated Roadway Conditions. *International Journal of Geo-Information, 14*(357), 1-25.

Ridolfi, E., Buffi, G., Venturi, S., & Manciola, P. (2017). Accuracy analysis of a dam model from drone surveys. *Sensors, 17*(8), 1777.

Roberts, R., Inzerillo, L., & Di Mino, G. (2020). Using UAV based 3d modelling to provide smart monitoring of road pavement conditions. *Information, 11*(12), 1–24.

Roca, D., Lagüela, S., Díaz-Vilariño, L., Armesto, J., & Arias, P. (2013). Low-cost aerial unit for outdoor inspection of building façades. *Automation in Construction, 36*, 128–135.

Russo, M., Carnevali, L., Russo, V., Savastano, D., & Taddia, Y. (2019). Modeling and deterioration mapping of façades in historical urban context by close-range ultra-lightweight UAVs photogrammetry. *International Journal of Architectural Heritage, 13*(4), 549–568.

Sanz-Ablanedo, E., Chandler, J. H., Rodríguez-Pérez, J. R., & Ordóñez, C. (2018). Accuracy of Unmanned Aerial Vehicle (UAV) and SfM photogrammetry survey as a function of the number and location of ground control points used. *Remote Sensing, 10*(10), 1606.

Turk, T., Bahadur, B., Demirel, Y., Altuntas, C., Ocalan, T. (2025). Investigation of the effect of GCP number and distribution on photogrammetric product accuracy in UAV photogrammetry. *Journal of Geodesy and Geoinformation, 12*(1), 77-88.

Vacca, G., Dessì, A., & Sacco, A. (2017). The use of nadir and oblique UAV images for building knowledge. *ISPRS International Journal of Geo-Information, 6*(393), 1–26.

Varbla, S., Puust, R., & Ellmann, A. (2021). Accuracy assessment of RTK-GNSS equipped UAV conducted as-built surveys for

construction site modelling. *Survey Review, 53*(381), 477–492.

Waagen, J. (2019). New technology and archaeological practice. Improving the primary archaeological recording process in excavation by means of UAS photogrammetry. *Journal of Archaeological Science, 101*, 11–20.

Watanabe, Y., & Kawahara, Y. (2016). UAV Photogrammetry for Monitoring Changes in River Topography and Vegetation. *Procedia Engineering, 154*, 317–325.

Yang, M. Der., Chao, C. F., Huang, K. S., Lu, L. Y., & Chen, Y. P. (2013). Image-based 3D scene reconstruction and exploration in augmented reality. *Automation in Construction, 33*, 48–60.

Zhang, D., Watson, R., Dobie, G., MacLeod, C., Khan, A., & Pierce, G. (2020). Quantifying impacts on remote photogrammetric inspection using unmanned aerial vehicles. *Engineering Structures, 209*(109940), 1–13.

Zhao, S., Kang, F., Li, J., & Ma, C. (2021). Structural health monitoring and inspection of dams based on UAV photogrammetry with image 3D reconstruction. *Automation in Construction, 130*(103832), 1–16.

URL-1: https://novatel.com/products/waypoint-post-processing-software/grafnav-static (Accessed: 21 March 2025).

URL-2: https://www.dji.com/global/phantom-4?site=brandsite&from=insite_search (Accessed: 02 April 2025).

URL-3: https://support.pix4d.com/hc/en-us/articles/209960726-Types-of-mission-Which-type-of-mission-to-choose-PIX4Dcapture (Accessed: 04 April 2025).

URL-4: https://leica-geosystems.com/products/total-stations/robotic-total-stations/leica-ts16 (Accessed: 17 February 2025).

URL-5: https://www.cloudcompare.org/main.html (Accessed: 20 April 2025).